Synthesis and Photoluminescence of $Cd_{1-x}Mn_xS$ ($x \leq 5\%$) Nanocrystals

G. Counio, T. Gacoin, and J. P. Boilot*

Laboratoire de Physique de la Matière Condensée, CNRS UMR 7643, École Polytechnique, 91128 Palaiseau Cedex, France

Received: December 11, 1997; In Final Form: March 17, 1998

We report the synthesis of $Cd_{1-x}Mn_xS$ nanocrystals with $x \leq 5\%$. Special care is taken to determine the final manganese concentration in the nanoparticles. The variation of the photoluminescence spectrum of $Cd_{1-x}Mn_xS$ colloidal solutions as a function of manganese concentration is studied. Characteristic luminescence features such as emission maximum wavelength and lifetime are analyzed. We find that it is possible to isolate contributions from particles containing no, one, or more Mn^{2+} ions. Dopant distribution among the crystallites is random and obeys to a binomial law. The agreement with this simple statistical model allows to use simple photoluminescence experiments to determine Mn^{2+} mean concentration and dispersion in $Cd_{1-x}Mn_xS$ nanocrystals.

I. Introduction

The II−VI semiconductors with Mn^{2+} ions homogeneously dispersed within their cationic network present interesting optical properties.[1] For example, high band gap materials such as CdS or ZnS with low Mn content (<1%) are well-known to exhibit a bright orange luminescence, characteristic of the $^4T_1 \rightarrow {}^6A_1$ transition of the Mn^{2+} 3d electron shell configurations. On the other hand, low band gap semiconductors such as CdTe or HgTe with high Mn content (>1%) exhibit interesting magnetooptical properties such as giant Faraday rotations.[2] These properties are a consequence of a strong exchange coupling between the localized moments of the paramagnetic dopant and the band electrons of the semiconductor.

It is also well-known that semiconductors having their dimensions in the nanometer range show a drastic change of their properties compared to the bulk materials. A huge amount of work exists on the quantum size effect, especially in the case of II−VI semiconductors such as CdS or CdSe. An interesting issue is then to study to what extent the quantum confinement affects the specific properties of II−VI compounds containing Mn^{2+} ions in solid solution.

Previous papers have described the synthesis of $Cd_{1-x}Mn_xS$ and $Zn_{1-x}Mn_xS$ nanoparticles.[3−6] In most cases, the processes involve a colloidal synthesis based on the simultaneous precipitation of both CdS (or ZnS) and MnS. A major difficulty concerns the precise determination of the manganese concentration effectively incorporated in the chalcogenide lattice. Indeed, all studies have concluded that only a small fraction of the initial manganese concentration is incorporated in the crystallites during the synthesis. Large excess of Mn^{2+} ions are then still present, surrounding of the particles as unreacted salts (possibly oxidized) or MnS precipitates. Consequently, if all the undesirable byproducts are not previously separated from the particles, a raw chemical analysis leads to an overestimation of the Mn content.

In a previous work,[5] we studied the synthesis and luminescence properties of $Cd_{1-x}Mn_xS$ nanoparticles, obtained by coprecipitation in reverse micelles solutions. Special care was taken when characterizing the Mn content by ESR, after carefully washing the particles in acidic water. We found that, within our experimental conditions, only a small amount of Mn can be incorporated so that most particles (2 nm in diameter) contain no more than a single Mn ion. We note that our results are in contrast with those reported by the group of Piléni,[7] who found it possible to incorporate up to 30% Mn, using the same process with slightly different experimental conditions.

In this paper, we investigate the luminescence properties of $Cd_{1-x}Mn_xS$ nanoparticles with x up to 5%. The particles are obtained following an original process, and special care was taken for the accurate determination of the mean Mn concentration x effectively incorporated into the CdS network. The photoluminescence spectrum of each sample appears as drastically dependent on its Mn concentration. By using a simple model, we establish a direct relationship between the luminescence properties and the distribution of Mn concentration in the nanoparticles. This provides a simple and accurate way to analyze Mn concentration and distribution within $Cd_{1-x}Mn_xS$ crystallites, without perturbative effects due to manganese ions located outside the nanoparticles.

II. Experimental Section

II.1. Apparatus. ESR experiments were performed on a Bruker ER200D instrument equipped with an Oxford continuous flow cryostat.[8] UV−visible absorption experiments were performed at room temperature with a Shimadzu UV-160A spectrophotometer. Photoluminescence, excitation, and phosphorescence spectra (recorded 2 ms after the extinction of the excitation) were performed at room temperature on $Cd_{1-x}Mn_xS$ colloidal solutions in methanol using a Hitachi F-4500 fluorescence spectrophotometer. Quantum yield evaluations were made by comparing the integrated intensity of the luminescence of our samples with those of standards of known efficiency taken under exactly the same conditions.[9]

II.2. Synthesis. In a first step, the precipitation of the particles is achieved in ethylene glycol by the simple mixing of one solution containing cadmium and manganese acetate and the other containing sodium sulfide. The cadmium concentration is constant equal to 0.1 mol·L^{-1}, and the manganese concentration is varied from 0 to 0.4 mol·L^{-1}. The sulfide

S1089-5647(98)00511-2 CCC: $15.00
Published on Web 06/17/1998

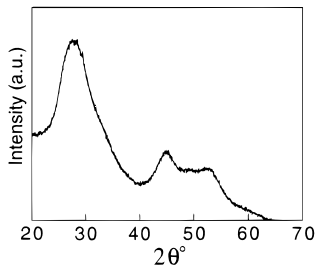

Figure 1. Typical X-ray diffraction pattern (Cu Kα) of $Cd_{1-x}Mn_xS$ nanocrystallites powder.

concentration is stoichiometric. A turbid yellow-orange suspension is obtained, consisting of partially agglomerated crystallites.

The solution is centrifuged and washed two times with methanol. The deagglomeration of the particles into a clear colloid is then obtained through the thermal treatment of the precipitate for 1 h in triethyl phosphate at 215 °C. The disjunction of the particles occurs through the grafting of phosphate molecules at the surface of the particles.[10] The detailed mechanism of this process, investigated in the case of pure CdS and CdSe nanoparticles, will be described in a separate paper.

After the heat treatment, the obtained colloidal solution can be destabilized upon the addition of heptane in excess. The flocculate is then washed two more times with heptane, and the resulting powder can be dispersed in methanol with high concentrations (>1 mol·L^{-1}). Further incorporation of the particles in sol−gel silica matrices can be achieved using the process we have already described in a previous work.[9]

The mean size of $Cd_{1-x}Mn_xS$ crystallites was deduced from X-ray diffraction experiments. A typical diffraction pattern is presented Figure 1. Best fits of the diffraction peaks located between $2\theta = 40°$ and 60° were obtained for a sphalerite structure and a coherence length of 2.4 nm, as determined using Scherrer's law.[12] This size was found to be nearly constant whatever the sample is, which suggests that the size distribution is not drastically dependent on the Mn content. Note also that for $x = 0\%$, this is in accordance with the value (2.5 nm) deduced from the optical band gap, using size/gap correlations previously reported for pure CdS nanocrystals.[13]

II.3. Determination of the Mean Mn concentration in the Nanocrystals. In order to determine exactly the concentration of Mn ions actually incorporated in $Cd_{1-x}Mn_xS$ particles, the powder is first extensively washed in pH 2.5 water. This allows the total dissolution of all other Mn products surrounding the particles as checked by ESR experiments.[14]

Figure 2 compares the ESR spectra of $Cd_{1-x}Mn_xS$ nanoparticles as obtained and after extensive acidic washing. Before washing, the signal is composed of an intense broad band and weaker narrow bands difficult to resolve. The broad signal originates mostly from Mn^{2+} ions in antiferromagnetic interaction. The narrow bands can be divided into two sets. The first one is characteristic of Mn^{2+} ions in an octahedral environment (hyperfine coupling constant $A_{iso} \approx 9$ mT) and probably arises from unreacted manganese ions. The second one is characteristic of Mn^{2+} ions located in a tetrahedral site ($A_{iso} \approx 7$ mT), and attributed to manganese ions incorporated in the CdS lattice.

After acidic washing, the intensity of the ESR spectra roughly decreases by 1 order of magnitude. In the case of a low initial manganese concentration, the ESR spectrum is composed of six narrow lines superimposed on a broad band. The six narrow bands ($g \approx 2$ and $A_{iso} = 6{,}9$ mT) originate from manganese ions in a tetrahedral environment, inside CdS nanocrystals. Two

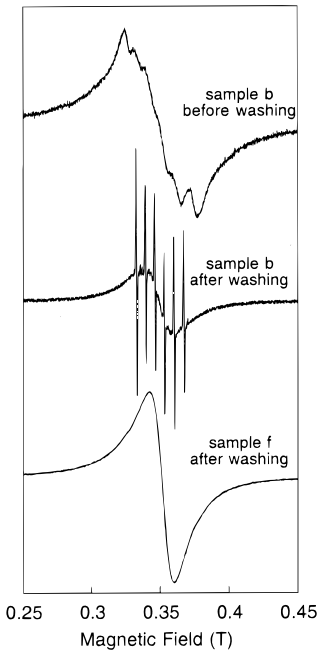

Figure 2. ESR evidence of parasitic magnetic phase elimination through acidic washing of as-obtained $Cd_{1-x}Mn_xS$ nanocrystals. Before washing: as-obtained crystallites, spectrum recorded at room temperature and with microwave power $P = 25$ mW. After washing: ESR spectra of sample b, $[Mn^{2+}]_{initial} = 0.05$, and sample f, $[Mn^{2+}]_{initial} = 0.3$ mol·L^{-1} after 18 h washing in pH 2.5 water in order to eliminate Mn byproducts of the synthesis. Spectra recorded at room temperature and microwave power $P = 25$ mW. The sample names are given in reference to Figure 4.

hypotheses can explain the broad ESR band observed underneath: it may originate either from isolated Mn^{2+} ions in perturbed environments[5] or from Mn^{2+} ions in antiferromagnetic interaction in a single nanoparticle. In the case of high initial manganese concentration, the ESR spectrum after washing only consists of a broad, slightly dissymmetric band, mostly due to antiferromagnetic interactions between paramagnetic centers in the crystals. In all cases, the extensive acidic washing leads to a significant decrease of the intensity and the disappearance of signals corresponding to octahedral manganese ions.

The manganese concentration in the crystallites is determined as the molar ratio of Mn^{2+} and S^{2-} ions per mass unit of the samples (assuming a stoichiometric composition). The Mn^{2+} concentration is determined by first dissolving a known mass of $Cd_{1-x}Mn_xS$ powder in concentrated acid and then comparing the ESR signal intensity with the signal of a reference.[8] The sulfur concentration is measured using the colorimetric method proposed by Mecklenburg et al.[15]

The results obtained for different starting Mn^{2+} concentrations are reported in Table 1. Under our experimental conditions, the maximum amount of Mn we found it possible to incorporate is $x = 5\%$. When this value is reached, the ratio of Mn incorporated inside the CdS to the initial Mn ions is about 7%. Although still small, this incorporation efficiency is much higher than the one we found in our previous study in inverted micelles (about 1%).[5] The interpretation of these results is difficult due to the complexity of the coprecipitation process. Nevertheless, solvating the metallic ions with ethylene glycol instead of water prevents the formation of oxo/hydroxo Mn complexes. Moreover, the chelating properties of ethylene glycol may also damp the high difference of solubility between MnS and CdS observed in bulk water,[16] greatly unfavorable in the case of simple aqueous coprecipitations.

TABLE 1: Total Quantum Efficiency η_{total} (%) and Quantum Efficiency of the Bands Detected at 1.9, 2.16, and 1.77 eV for x_{Mn} Ranging from 0 to 4.8%[a]

sample	x_{Mn} (%)	N_{Mn}	$\eta_{1.9\ eV}$ (%)	$\eta_{2.16\ eV}$ (%)	$\eta_{1.77\ eV}$ (%)	η_{total} (%)
a	0	0	≈1	0.0	0.0	≈1
b	0.8	1.0	−	19.5	−	20.5
c	1.3	1.6	0.2	12.0	1.4	13.6
d	2.5	3.1	0.0	6.1	2.0	8.1
e	3.9	4.9	0.0	2.9	1.8	4.7
f	4.8	6.0	0.0	2.0	1.4	3.4

[a] Assuming an average diameter of 2.5 nm in all the samples, CdS nanoparticles contain about 300 atoms (Cd + Mn + S).[19] The mean number of manganese per particle N_{Mn} is then determined by $N_{Mn} = 150x_{Mn}$. Dashes mean that the quantum yield could not be correctly measured because the other luminescence contributions are too intense. The sample names are given in reference to Figure 4.

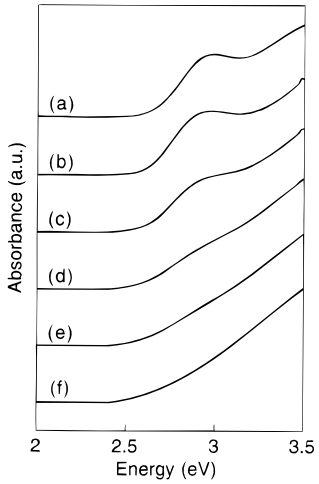

Figure 3. UV−visible absorption spectra of various $Cd_{1-x}Mn_xS$ colloidal solutions in methanol. Sample names are given in reference to Figure 4.

III. Optical Properties

Figure 3 shows the UV−visible absorption spectra of $Cd_{1-x}Mn_xS$ colloids. By increasing Mn content, we note a progressive slight red shift of the energy threshold (up to about 0.1 eV). Besides, the excitonic structure is gradually damped, and totally vanishes for highly doped particles. These results may be interpreted either as a broadening of the Mn distribution between the particles or as a broadening of the size distribution. Electron microscopy experiments were performed on samples a and f, and the standard deviation of each size distribution was found to be 0.75 and 0.61, respectively. Nevertheless, we must note that the accuracy of this determination is hardly limited by the difficulty to observe the smallest particles. Considering now the red shift of the absorption threshold, we find that it is almost consistent with the expected variation of the band gap for the bulk phase in the same Mn composition (from $x = 0$ to $x = 5\%$).[17] In this case, one can reasonably assume that the damping of the excitonic structure in the absorption spectra is directly related to a broadening of the Mn distribution when the average Mn content of each sample increases.

The evolution of the photoluminescence spectra of six $Cd_{1-x}Mn_xS$ samples with increasing average manganese concentration is presented in Figure 4 a−f. Three main contributions are observed, whose relative intensity changes with the Mn content:

The first contribution is a very broad band centered at about 1.9 eV. The lifetime of this band, measured in a previous work,[6] varies with the detection energy but always falls in the microsecond time scale. This band is commonly observed in pure CdS nanocrystals (i.e., with no Mn) and is thought to originate from deep surface trap recombinations.

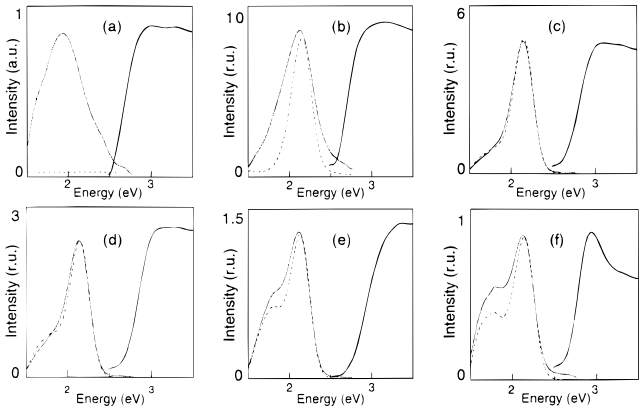

Figure 4. Photoluminescence, excitation (plain lines), and phosphorescence (dotted lines) spectra of $Cd_{1-x}Mn_xS$ colloidal solutions in methanol with various x_{Mn}: 0 (a), 0.008 (b), 0.013 (c), 0.025 (d), 0.039 (e), 0.048 (f). The spectra are recorded peak to peak. The intensities of spectra b−f are given relative to spectrum a.

The second contribution is a phosphorescence band peaking at 2.16 eV. Its lifetime is 1.7 ms at room temperature.[6] In our samples, its maximum intensity is reached for an average Mn concentration of about 0.8%. As already shown by previous works, this contribution is characteristic of the Mn^{2+} internal $^4T_1 \rightarrow {}^6A_1$ transition. In the case of bulk compounds, its highest quantum efficiency is observed when the Mn^{2+} ions are infinitely diluted.[1]

The third contribution is a phosphorescence band centered at about 1.77 eV. Its lifetime is found to be in the millisecond time scale. As in the bulk materials,[18] this recombination is believed to occur after the capture of the excitation energy by so-called "red emission centers". It is still not clear whether these centers are Mn^{2+} pairs and/or Mn^{2+} ions located in perturbed environments.

Table 1 gives an estimation of the quantum yield measured for each contribution taken independently. We can see that the intensity of the first contribution is maximum for no Mn present in the nanocrystals, the intensity of the second band is maximum for about one Mn per nanocrystal, and the relative intensity of the third band rises for higher Mn content, while the global emission intensity vanishes. These observations strongly suggest that there must be a correlation between the statistic repartition of Mn among the particles of a given sample and its luminescence spectrum.

In a simple model, we neglect the size distribution of the particles, and we consider that during the synthesis of the particles, the incorporation of the Mn ions in the nanocrystals occurs randomly. The distribution of Mn ions among the particles obeys a binomial law: the model developed by Lippens et al.[19] roughly estimates as 150 the number of metallic sites in a 2.4 nm diameter CdS nanoparticle. If x is the mean manganese concentration, the probability law $p(\tilde{N}_{Mn})$ ruling the number of Mn^{2+} ions per nanocrystal $\tilde{N}_{Mn}$, is

$$p(\tilde{N}_{Mn}) = \binom{150}{\tilde{N}_{Mn}} x^{\tilde{N}_{Mn}} (1-x)^{150-\tilde{N}_{Mn}}$$

where

$$\binom{n}{m}$$

is a binomial coefficient.

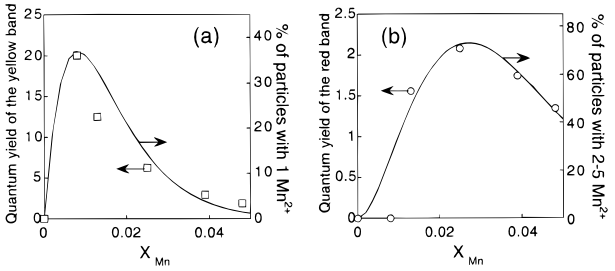

Figure 5. Correlation between the quantum yield (markers) and the proportion of particles with a given number of Mn^{2+} ions if a binomial distribution is assumed (plain line).

Using this law, we can calculate the exact number of particles having 1 Mn as a function of the average Mn concentration in the samples. Results are plotted in Figure 5a, and compared to the experimental values of the quantum yield of the yellow luminescence. A good agreement is observed between experimental luminescence efficiencies and calculated nanoparticles population ratio. This suggests that the intense yellow luminescence band originates from crystallites containing exactly one Mn^{2+} ion, i.e., corresponding to the infinitely diluted case. In fact, it does not mean that particles containing two isolated Mn^{2+} cannot emit this yellow luminescence. But this last contribution is almost negligible because the corresponding high Mn concentration in the bulk material (about 2%) does not produce a significant contribution to the yellow band.[1]

The ratio of the quantum yield of a sample to the proportion of such particles also allows to extract the photoluminescence quantum yield of particles with one Mn. The result is roughly equal to 60%, and almost independent of the sample for which the calculation is performed.

The same analysis has been applied to the red luminescence band (Figure 5b). We assume that this luminescence band originates from particles containing more than one Mn and receives the same contribution from each particle. Nevertheless, high manganese concentration favors nonradiative recombination processes. This effect is taken into account by setting a cutoff: the best agreement between experimental luminescence efficiencies and calculated nanoparticles population ratio is reached when particles containing 6 Mn^{2+} ions or more are considered nonluminescent and discarded. The same calculation as before gives an average quantum yield of 1% for $Cd_{1-x}Mn_xS$ crystallites containing between 2 and 5 manganese ions.

Considering the average transition probability for the yellow and red contributions, the relative intensities of these two luminescence bands provide a fast and accurate tool to determine the mean Mn^{2+} concentration and the Mn^{2+} repartition in a sample of $Cd_{1-x}Mn_xS$ nanocrystals.

IV. Conclusion

In conclusion, we have described an original chemical process to elaborate $Cd_{1-x}Mn_xS$ nanoparticles (2.5 nm in diameter). The manganese concentration can be tuned up to $x = 5\%$. The luminescence spectrum of each sample is the sum of three individual contributions, whose characteristics are summarized in Table 2. Since the luminescence emitted by a particle is characteristic of the number of Mn^{2+} ions it contains, the relative intensities of these three contributions can be used to measure the mean concentration and the distribution of manganese ions among the particles. In our case, this distribution follows a binomial law, showing a random dispersion of Mn^{2+} in the CdS crystallites.

TABLE 2: Photoluminescence Characteristics of the Luminescence Bands Emitted by $Cd_{1-x}Mn_xS$ Nanocrystals[a]

	center (eV)	lifetime	quantum yield (%)	$\tilde{N}_{Mn}$
yellow/orange band	1.9	$\approx 3\ \mu s$[6]	1	0
yellow band	2.16	1.7 ms[6]	60	1
red band	1.77	>1 ms	1	2−5

[a] The center and lifetime are experimental results. The interpretation of the variations of the photoluminescence spectra of the colloids with x_{Mn} with a statistical model allows to assign each contribution to a population of crystals containing a given number of manganese $\bar{N}_{Mn}$. The quantum yield is then calculated as the ratio of the efficiency of each band to the proportion of nanoparticles having $\tilde{N}_{Mn}$ manganese centers.

References and Notes

(1) Goede, O.; Heimbrodt, W. *Phys. Stat. Sol. (b)* **1988**, *146*, 11.
(2) Gaj, J. A.; Galazka, R. R.; Nawrocki, M. *Solid State Commun.* **1978**, *25*, 193.
(3) Wang, Y.; Herron, N.; Moller, K.; Bein, T. *Solid State Commun.* **1991**, *77*, 33. Khosravi, A. A.; Kundu, M.; Kuruvilla, B. A.; Shekhawat, G. S.; Gupta, R. P.; Sharma, A. K.; Vyas, P. D.; Kulkarni, S. K. *Appl. Phys. Lett.* **1995**, *67* (17), 506. Jin, C.; Hou, S.; Dou, K.; Chen, Y.; Huang, S.; Yu, *J. Chin. Sci. Bull.* **1995**, *40* (21), 1782. Sooklal, K.; Cullum, B.; Angel, S. M.; Murphy, C. *J. Phys. Chem.* **1996**, *100*, 4551.
(4) Bhargava, R. N.; Gallagher, D.; Hong, X.; Nurmikko, A. *Phys. Rev. Lett.* **1994**, *72* (3), 416.
(5) Counio, G.; Esnouf, S.; Gacoin, T.; Boilot, J. P. *J. Phys. Chem.* **1996**, *100*, 20021.
(6) Chamarro, M. A.; Voliotis, V.; Grousson, R.; Lavallard, P.; Gacoin, T.; Counio, G.; Boilot, J. P.; Cases, R. *J. Cryst. Growth* **1996**, *159*, 853.
(7) Levy, L.; Hochepied, J. F.; Pileni, M. P. *J. Phys. Chem.* **1996**, *100*, 18322.
(8) Manganese acetate aqueous solution in concentrated acid was used as an intensity reference.
(9) Drexhage, K. H. *Dye Lasers, Topics in Applied Physics Vol. 1*; F. P. Schäfer, Ed.; Springer-Verlag: Berlin, 1973−1977.
(10) Such strong interaction was demonstrated by Murray et al. in the case of trioctylphosphine oxide. Murray, C. B.; Norris, D. J.; Bawendi, M. G. *J. Am. Chem. Soc.* **1993**, *115*, 8706.
(11) Gacoin, T.; Train, C.; Chaput, F.; Boilot, J. P.; Aubert, P.; Gandais, M.; Wang, Y.; Lecomte A. *Sol−Gel Optics II*; SPIE Proc. 1758; SPIE: San Diego, CA, 1992; p 565.
(12) Guinier, A. *Théorie et technique de la radiocristallographie*, 3rd ed.; Dunod: Paris, 1964.
(13) Wang, Y.; Herron, N. *Phys. Rev. B* **1990**, *42* (11), 7253.
(14) Counio, G. Thèse de Doctorat, École Polytechnique 1997.
(15) Mecklenburg, W.; Rosenkranzer, F. *Z. Anorg. Chem.* **1914**, *86*, 143.
(16) Bjerrum, J. *Solubility Constants Pt. II: Inorganic Ligands*; The Chemical Society, London, 1958.
(17) Ikeda, M.; Itoh, K.; Kisano S. *J. Phys. Soc. Jpn.* **1968**, *25*, 455.
(18) Goede, O.; Thong, D. D. *Phys. Stat. Sol. (b)* **1984**, *81*, 343.
(19) Lippens, P. E.; Lanoo, M. *Phys. Rev. B* **1989**, *39*, 10935.